Numerical simulation of *ac* transport in graphene on a SiO2 substrate

N. Sule*, K. J. Willis, S. C. Hagness, and I. Knezevic
Electrical and Computer Engineering Department
University of Wisconsin-Madison
Madison WI, USA
*sule@wisc.edu

Abstract— **We calculate the complex conductivity of graphene in the terahertz (THz) to mid-infrared (mid-IR) frequency range using a numerical simulation that couples the two-dimensional (2D) ensemble Monte Carlo technique (EMC) for carrier transport, the three-dimensional (3D) finite-difference time-domain (FDTD) technique for electrodynamics, and molecular dynamics (MD) for short range Coulomb interactions. We demonstrate the effect of the typically used silicon-dioxide substrate on the high-frequency carrier dynamics in graphene and show good agreement between recent experimental results and our numerical simulations.**

Keywords-graphene; electron transport; terahertz; conductivity

I. INTRODUCTION

Graphene is a promising material for novel electronic and optoelectronic device applications [1]–[3]. Although considerable work has been done on the fundamental electronic properties [4] and low-field *dc* transport [5] in graphene, high-frequency carrier dynamics in this material has not been extensively studied [6]. From a technological perspective, the application of graphene in optoelectronic devices, such as transparent conductors, photodetectors, and metamaterials, requires a deeper understanding of the interaction of high-frequency electromagnetic waves with the carriers in this two-dimensional system. Moreover, the effect of a substrate and the impurities therein cannot be ignored for device applications.

II. NUMERICAL MODEL

Here, we calculate the frequency-dependent conductivity of graphene and demonstrate the effect of a typical SiO2 substrate on the carrier dynamics. Our numerical simulation combines the ensemble Monte Carlo (EMC) technique for solving the Boltzmann transport equation for carrier transport in the two-dimensional (2D) graphene layer with the three-dimensional (3D) finite-difference time-domain (FDTD) technique [7] for solving Maxwell's curl equations throughout the domain. The short-range Coulomb forces exerted on the carriers by impurity ions are calculated using molecular dynamics (MD). The EMC, FDTD, and MD solvers are coupled in each time step, such that the combined FDTD-MD fields accelerate the carriers and the EMC carrier motion produces the sourcing current density. This coupled EMC-FDTD-MD technique has previously been used to accurately calculate the *ac* conductivity of doped silicon [8], [9].

The simulation domain, as shown in Fig. 1a, consists of a monolayer graphene sheet with air on top and a SiO2 substrate at the bottom, with dielectric constants of $\varepsilon_g = 2.5$, $\varepsilon_a = 1.0$, and $\varepsilon_s = 3.9$, respectively. We use periodic boundary conditions for the bounding planes perpendicular to the plane of carrier transport (the *xz* and *yz* planes in Fig. 1a), in order to simulate a very large sheet of graphene. The simulation domain is terminated with convolutional perfectly matched layer (CPML) boundary conditions [7] on the top and bottom boundaries. The initial electric field distribution due to the carriers and charged impurities is shown in Fig. 1b.

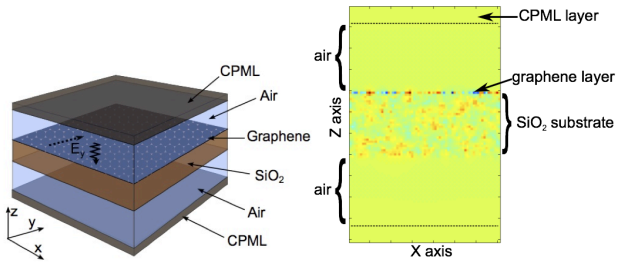

(a) Model geometry (b) Field distribution

Figure 1. (a) 3D EMC-FDTD model geometry. The wavy arrow denotes the direction of propagation of the wave, while the dotted arrow shows the direction of the electric field. The domain boundaries perpendicular to *x* and *y* are terminated by periodic boundary conditions. (b) Visualization of the spatial distribution of the electric field (E_y) stemming from the influence of the carriers in the graphene sheet and the charged impurities in the SiO2 substrate at the start of the simulation.

The 2D carrier transport is limited by the Coulomb fields of the impurities in the substrate, in addition to scattering with longitudinal acoustic (LA) and optical (LO) phonons, as well as polar surface optical (SO) phonons due to the substrate. The LA and LO scattering rates are calculated using the tight-binding Bloch (TBB) wave functions and are fitted to *ab-initio* electron-phonon scattering rates to deduce the deformation potentials [10]. The SO scattering rates are calculated based on the interaction Hamiltonian from Ref. [11], and the TBB wave functions.

ISBN 978-0-615-71756-2

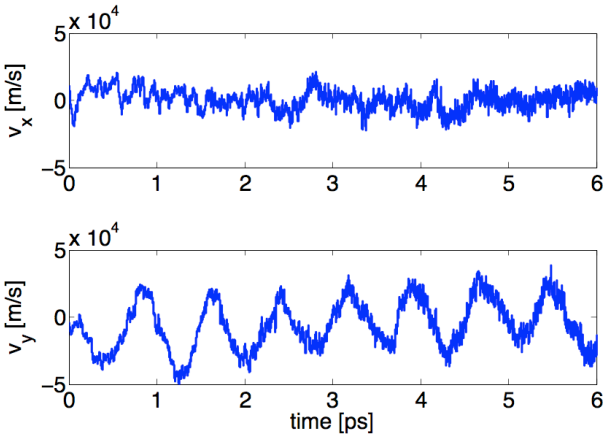

Figure 2. Time evolution of the average carrier velocity for a 13 THz plane wave excitation with electric field along the *y-direction* (as shown in Figure 1). Carrier density is 6.3×10^{12} cm^{-2} and the ensemble contains around 10,000 carriers. Transport in this case is limited by LO, LA, and SO scattering in addition to the Coulomb impurity interaction.

III. Results

Ensemble averages of the drift velocity, carrier density, and energy are calculated at each time step. Fig. 2 shows the time evolution of the carrier velocity for a 13 THz plane wave excitation, with electric field along the *y-direction*. Current density and electric field phasors are calculated using fast Fourier transform after a steady state has been reached, and are used to calculate complex conductivity. In Fig. 3, we show the real part of the $|E(\omega)|^2$ complex conductivity as a function of frequency for supported and unsupported (suspended) graphene with a carrier density of 6.3×10^{12} cm^{-2}. We contrast transport in a suspended graphene sheet, where the intrinsic LA and LO phonon-electron scattering limits carrier dynamics, with transport in supported graphene, where the inclusion of SO phonon-electron and impurity scattering is necessary. A significant effect on the conductivity of graphene due to the SO phonons (red squares) as well as the impurities (green diamonds and pink triangles) is clearly seen in Fig. 3. For example, the conductivities of suspended graphene (blue squares) at 4 THz ($\mathrm{Re}\{\sigma\} = 3.8$ e^2/h) and 10 THz ($\mathrm{Re}\{\sigma\} = 1.6$ e^2/h) are lower than those of supported graphene without impurities (red squares) by factors of 6 and 3, respectively. In contrast, at frequencies below 1 THz, the conductivity of suspended graphene exceeds that of supported graphene. We find good agreement with the experimental data [6] (black curve) corresponding to the same carrier density tuned via a gate voltage of 50 V, for a simulation with an impurity density that is twice the carrier density.

IV. Conclusion

In conclusion, we have calculated the complex conductivity of graphene in the THz to mid-IR frequency range by simulating the high frequency carrier dynamics using a coupled EMC-FDTD-MD numerical solver. We demonstrate that the substrate has a significant influence on carrier transport at low frequencies, while its influence becomes less pronounced at frequencies greater than 10 THz. Our results show good agreement with recent experimental data [6] for practically relevant carrier and substrate impurity densities. Moreover, we can independently tune the impurity density and also predict the frequency dependent conductivity of graphene supported on an ideally clean SiO2 substrate. Such a characterization of the high-frequency conductivity of supported and gated graphene might provide useful for photonic and optoelectronic device applications.

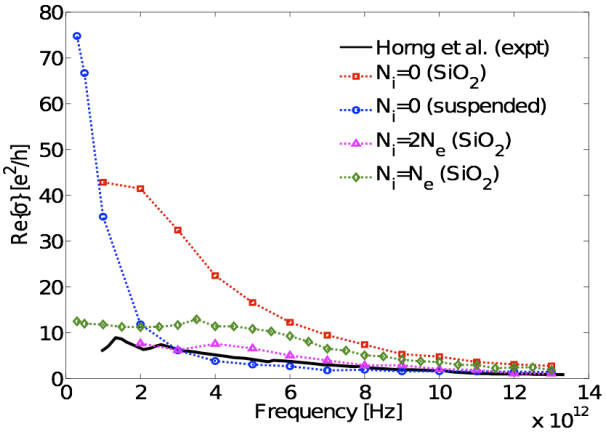

Figure 3. The real part of the complex conductivity of graphene as a function of frequency at the carrier density of $N_e = 6.3 \times 10^{12}$ cm^{-2}, which is the same density for a gate voltage of 50 V in [6]. Blue circles denote suspended graphene without impurities, red squares denote graphene on SiO2 substrate without impurities, green diamonds and pink triangles denote different impurity levels in supported graphene, and the black solid curve corresponds to the experimental data from Horng et al. (Ref. [6]). Good agreement with experimental data is found for impurity density exceeding the electron density twofold ($N_i = 2N_e$.)

Acknowledgment

This work has been supported by the NSF through the University of Wisconsin MRSEC (award DMR-0520527), and by the AFOSR (awards FA9550-09-1-0230 and FA9550-11-1-0299).

References

[1] Ph. Avouris, Z. Chen and V. Perebeinos. "Carbon-based electronics," *Nature Nanotech.* 2, pp. 605-615 (2007).

[2] A. K. Geim, and K. S. Novoselov. "The rise of graphene," *Nature Mater.* 6, pp. 183-191 (2007).

[3] F. Bonaccorso, Z. Sun, T. Hasan, and A. C. Ferrari. "Graphene photonics and optoelectronics," *Nature Photon.* 4, pp. 611-622 (2010).

[4] A. H. Castro Neto, F. Guinea, N. M. R. Peres, K. S. Novoselov, and A. K. Geim. "The electronic properties of graphene," *Rev. Mod. Phys.* 81, pp. 109-162 (2009).

[5] S. Das Sarma, Shaffique Adam, and E. H. Hwang. "Electronic transport in two-dimensional graphene," *Rev. Mod. Phys.* 83, pp. 407-470 (2011).

[6] J.Horng et al."Drude conductivity of Dirac fermions in graphene," *Phys. Rev. B* 83, 165113 (2011).

[7] A. Taflove and S. C. Hagness. *Computational Electrodynamics: The Finite-Difference Time-Domain Method,* 3rd ed., Artech House, 2005.

[8] K. J. Willis, S. C. Hagness and I. Knezevic. "Terahertz conductivity of doped silicon calculated using ensemble Monte Carlo/finite-difference

time-domain (EMC/FDTD) simulation technique," *Appl. Phys. Lett.* 96, 062106 (2010).

[9] K. J. Willis, S. C. Hagness and I. Knezevic. "Multiphysics simulation of high-frequency carrier dynamics in conductive materials," *J. Appl. Phys.* 110, 063714 (2011).

[10] N. Sule and I. Knezevic. "Phonon-limited electron mobility in graphene calculated using tight-binding Bloch waves," submitted to *J. Appl. Phys.* (2012).

[11] A. Konar, T. Fang and D. Jena. "Effect of high-κ dielectrics on charge transport in graphene-based field effect transistors," *Phys. Rev. B* 82, 115452 (2010).